

# Doped $t$ - $J$ Model on a Triangular Lattice: Possible Application to $\text{Na}_x\text{CoO}_2 \cdot y\text{H}_2\text{O}$ and $\text{Na}_{1-x}\text{TiO}_2$

Qiang-Hua Wang<sup>a</sup>, Dung-Hai Lee<sup>b</sup>, and Patrick A. Lee<sup>c</sup>

(a) National Laboratory of Solid State Microstructures,

Institute for Solid State Physics, Nanjing University, Nanjing 210093, China

(b) Department of Physics, University of California at Berkeley, Berkeley, CA 94720, USA and

(c) Department of Physics, Massachusetts Institute of Technology, Cambridge, MA 02139, USA

We report the finding of time-reversal-symmetry-breaking  $d_{x^2-y^2} + id_{xy}$  superconducting ground state in the slave-boson mean-field theory for the  $t$ - $J$  model on triangular lattice. For  $t/J = -5$  ( $t/J = -9$ ) pairing exists for  $x < 13\%$  ( $x < 8\%$ ) upon electron doping, and  $x < 56\%$  ( $x < 13\%$ ) upon hole doping. These results are potentially relevant to doped Mott insulators  $\text{Na}_x\text{CoO}_2 \cdot y\text{H}_2\text{O}$  and  $\text{Na}_{1-x}\text{TiO}_2$ .

There is now broad agreement that the physics of the high  $T_c$  cuprate is that of the doped Mott insulator. However, 17 years after its discovery[1] the layered cuprates remain the only materials which exhibit the phenomenon of high  $T_c$  superconductivity. There are three reasons which make the cuprates unique: (1) The parent compound is a Mott insulator with  $S = \frac{1}{2}$  and no orbital degeneracy; (2) the structure is two dimensional; and (3) the exchange energy  $J$  is very large ( $J \approx 1500$  K). Anderson[2] has stressed the strong quantum fluctuation of the  $S = \frac{1}{2}$  system in two dimensions. His resonating valence bond (RVB) theory describes a liquid of spin singlet which becomes a superconductor when the holes are phase coherent. If this is a general property of a doped Mott insulator, it will clearly be desirable to examine other examples which satisfy these three criteria. Recently Takada *et al.*[3] reported the discovery of superconductivity in  $\text{Na}_x\text{CoO}_2 \cdot y\text{H}_2\text{O}$  with a  $T_c$  of 5 K for  $x = 0.35$ . As these authors pointed out, this system may be viewed as a Mott insulator with electron doping of 35%. The Co atoms are in a triangular lattice and the  $\text{Co}^{4+}$  atom is in a low spin ( $S = \frac{1}{2}$ ) state. Thus this material satisfies the first two criteria listed above. The value of  $J$  is not known at present, but the new discovery offers hope that a second system which exhibits superconductivity by doping a Mott insulator may be realized. A summary of what is known about this material and a discussion in terms of RVB physics was given by Baskaran.[4] In this paper we argue that the  $t$ - $J$  model on a triangular lattice is a reasonable starting point to model these materials. We estimate the value of  $J$ , and compute the slave boson mean field phase diagram for both electron and hole doping. We find  $d_{x^2-y^2} + id_{xy}$  pairing over significant range of doping for both  $t/J = -5$  and  $t/J = -9$ . The appearance of superconductivity shows an interesting particle-hole asymmetry. We propose that  $\text{Na}_{1-x}\text{TiO}_2$  may be an example of the hole-doped system.

The transition metal oxide layers in  $\text{Na}_x\text{CoO}_2$  and  $\text{Na}_{1-x}\text{TiO}_2$  form a common structure where the transition metal is surrounded by an octahedral oxygen cage. The cages are edge sharing, forming a layered structure.

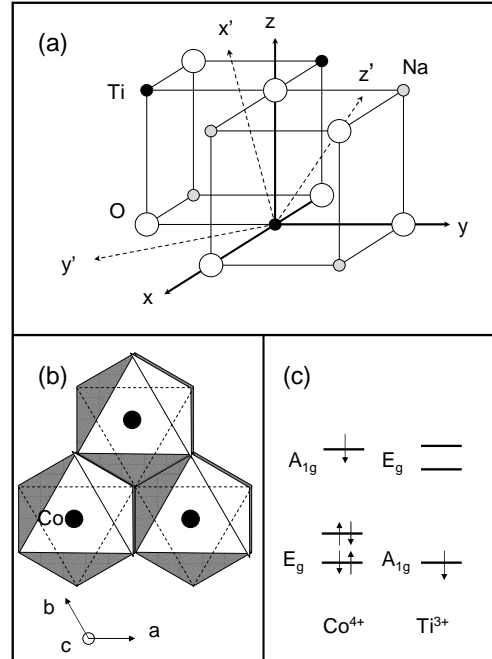


FIG. 1: (a) The  $\text{NaTiO}_2$  structure. (b) Projection of Fig.1(a) along the (1,1,1) direction showing the oxide layer. This layer is similar in  $\text{Na}_x\text{CoO}_2$  and  $\text{NaTiO}_2$ . Oxygen occupies vertices of the solid (dashed) triangles which lie above (below) the cobalt or titanium layers. (c) The splitting of the  $t_{2g}$  levels due to the distortion of the oxygen octahedra.

The stacking of the oxide layers is different in the two materials and we first describe the structure of  $\text{Na}_{1-x}\text{TiO}_2$ . A way to visualize the structure which is convenient for understanding the electronic structure is given in Fig.1(a) (adopted from Ref.[5]). It shows a piece of the crystal structure in a co-ordinate system which is standard for the oxygen octahedron. The hexagonal layered struc-

ture is visualized by looking down on this structure along the (1,1,1) direction. Thus the axis  $z'$  becomes the  $c$ -axis in the layered hexagonal structure notation. One can see stacking of O-Ti-O or O-Co-O hexagonal layers, highlighted in Fig.1(b), separated by a Na layer. In  $\text{Na}_{1-x}\text{TiO}_2$ , the Na sits directly over the oxygen in the layer below Ti (vertices of the dashed triangle), whereas in  $\text{Na}_x\text{CoO}_2$ , the Na site is on top of the Co. The next  $\text{CoO}_2$  layer has Co on top of Na but the stacking order of the oxygen layer is reversed (solid triangle now lies below Co) thereby doubling the unit cell along  $c$ . This difference in stacking does not affect the electronic structure of the  $\text{CoO}_2$  layers and will be ignored from now on.

From Fig.1(a) it is clear that the  $d$  states are split into  $t_{2g}$  and  $e_g$  orbitals by the octahedral environment. A shift of the oxygen along the (1,1,1) direction splits the  $t_{2g}$  orbitals into[5]

$$A_{1g} = (d_{xy} + d_{yz} + d_{zx})/\sqrt{3} \quad (1)$$

and a doublet (labelled  $E_g$  to distinguish from  $e_g$ )

$$E_g = ((d_{zx} - d_{yz})/\sqrt{2}, (-2d_{xy} + d_{yz} + d_{zx})/\sqrt{6}). \quad (2)$$

The band calculation of Singh[6] showed that the splitting is fairly large in  $\text{Na}_{0.5}\text{CoO}_2$  with  $A_{1g}$  lying higher than  $E_g$ . As shown in Fig.1(c), in  $\text{Co}^{4+}$  the unpaired spin occupies the non-degenerate  $A_{1g}$  orbital. We note that the  $t_{2g}$  orbitals have lobes which point to the mid-point of lines connecting the oxygens in the octahedral cage. From Fig.1(a) and Eq.(1) we see that the  $A_{1g}$  orbitals on nearest neighbor Co have components which point directly at each other. Thus unlike the cuprate, where the hopping is via the Cu-O covalent band, in the cobalt compounds, the direct overlap between the  $A_{1g}$  orbitals form a band. Due to band overlap, it is difficult to extract the  $A_{1g}$  bandwidth from Singh's calculations [6] but we estimate it to be between 1 to 1.4 eV. From this we extract the hopping integral  $t$  for the  $t$ - $J$  model

$$H = -t \sum_{\langle ij \rangle} \left( P c_{i\sigma}^\dagger c_{j\sigma} P + \text{h.c.} \right) + J \sum_{\langle ij \rangle} \left( \mathbf{S}_i \cdot \mathbf{S}_j - \frac{1}{4} n_i n_j \right) \quad (3)$$

to be  $t = -0.11$  to  $-0.15$  eV. In Eq. (3) the projection operator  $P$  removes double/zero occupancy for hole/electron doping respectively. We note that the overlap between  $A_{1g}$  orbitals is positive and the negative sign of  $t$  is a consequence of the sign convention chosen in Eq.(3). As emphasized by Baskaran,[4] there is no particle-hole symmetry in the triangular lattice and the sign of  $t$  is important. Singh's band structure [6] shows a maximum in the band structure at  $\Gamma$ , confirming the negative sign of  $t$ . The Fermi surface of  $\text{Na}_{0.5}\text{CoO}_2$  consists of a hole pocket of area  $\frac{1}{4}$  around the  $\Gamma$  point.[6] This is consistent with photoemission results.[7]

It is much more difficult to estimate the exchange constant  $J = 4t^2/U$  because the  $U$  parameter is highly uncertain due to screening. We appeal to another  $t_{2g}$   $S = \frac{1}{2}$

system where  $J$  has been determined experimentally. In  $\text{TiOCl}$  the  $t_{2g}$  orbital is orbitally ordered and forms one-dimensional  $S = \frac{1}{2}$  spin chains.[8] The exchange interaction was found to be 660 K by fitting the spin susceptibility to the Bonner-Fisher curve. In this case the  $t_{2g}$  orbitals are pure  $d_{yz}$  and point directly at each other. The bandwidth from band structure calculations is also about 1 eV, leading to  $t \approx -1/4$  eV. Note that  $t$  for  $\text{Na}_x\text{CoO}_2$  is considerably smaller even though the Co-Co distance at 2.84 angstrom is shorter than the Ti-Ti distance (3.38 angstrom). This is because only one component out of three in Eq.(1) points directly towards each other. Assuming that  $U$  is similar, our best guess for  $J$  is 12 to 24 meV and  $|t/J| \approx 6$  to 9. Note that our estimate of  $J$  for  $\text{Na}_x\text{CoO}_2$  is about an order of magnitude smaller than that for the cuprates.

It is interesting to consider another  $S = \frac{1}{2}$  system which corresponds to single occupation of the  $t_{2g}$  orbitals.  $\text{NaTiO}_2$  has similar layer structure as  $\text{Na}_x\text{CoO}_2$  but the Na layer is nominally fully occupied. The  $\text{Ti}^{3+}$  has  $d^1$  configuration giving rise to unpaired  $S = \frac{1}{2}$ . Contrary to  $\text{Na}_{0.5}\text{CoO}_2$ , the  $A_{1g}$ ,  $E_g$  splitting is much smaller than the bandwidth, according to LDA calculations.[5] However, an LDA+U calculation shows that the  $A_{1g}$  orbital is occupied preferentially, so that the single electron again occupies the nondegenerate  $A_{1g}$  band.[5] Reduction of the Na occupation ( $\text{Na}_{1-x}\text{TiO}_2$ ) corresponds to doping by  $x$  holes. The undoped system is of great interest because it is one of the few known examples of the  $S = \frac{1}{2}$  triangular antiferromagnet. However, the control of Na stoichiometry presents a serious materials challenge and relatively few studies have been carried out to date.[9]

As we mentioned earlier the occupation constraint of Eq. (3) is different for the electron and hole doping. In the case of electron doping we shall perform a particle-hole transformation  $c_{i,\sigma} \rightarrow c_{i,-\sigma}^\dagger$  so that the constraint always means no double occupancy and the sign of  $t$  is reversed. Consequently  $t < 0$  for hole-doped  $\text{Na}_{1-x}\text{TiO}_2$  and  $t > 0$  for electron-doped  $\text{Na}_x\text{CoO}_2$ .

The starting point of our calculation is the following U(1) slave-Boson mean-field Hamiltonian[10] for the t-J model at hand,  $H_{MF} = H_{nm} + H_m$  with

$$\begin{aligned} H_{nm} &= - \sum_{\langle ij \rangle \sigma} \left[ \left( t\sqrt{x_i x_j} + \frac{3J}{8} \chi_{ij}^* \right) f_{i\sigma}^\dagger f_{j\sigma} + \text{h.c.} \right] \\ &\quad - \frac{3J}{8} \sum_{\langle ij \rangle \sigma \sigma'} \left[ \Delta_{ij}^* f_{i\sigma} f_{j\sigma'} \epsilon_{\sigma \sigma'} + \text{h.c.} \right] - \sum_{i\sigma} \mu_i n_{i\sigma}; \\ H_m &= J \sum_{\langle ij \rangle} (\mathbf{S}_i \cdot \mathbf{m}_j + \mathbf{S}_j \cdot \mathbf{m}_i). \end{aligned} \quad (4)$$

Here  $x_i = 1 - \sum_{\sigma} \langle n_{i\sigma} \rangle$  and  $\mu_i$  is the corresponding local Lagrange multiplier. The doping level is given by  $x = \sum_i x_i/N$  with  $N$  the lattice sites. The mean field order parameters are  $\chi_{ij} = \sum_{\sigma} \langle f_{i\sigma}^+ f_{j\sigma} \rangle$ ,  $\Delta_{ij} = \sum_{\sigma \sigma'} \epsilon_{\sigma \sigma'} \langle f_{i\sigma} f_{j\sigma'} \rangle$ , and  $\mathbf{m}_i = \langle \mathbf{S}_i \rangle$  with  $\mathbf{S}_i =$

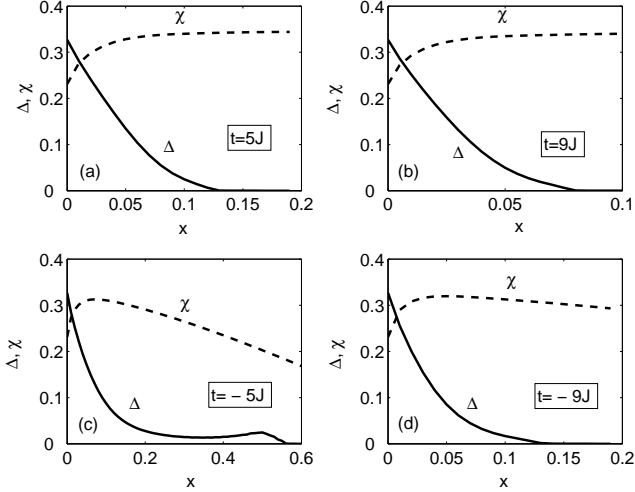


FIG. 2: Dependence of the order parameters on hole doping ( $x$ ):  $t = 5J$  (a),  $9J$  (b),  $-5J$  (c), and  $-9J$  (d). Note the scale change in 2(b) and 2(c).

$\sum_{ss'} \sigma_{ss'} f_{is}^\dagger f_{is'}/2$ . Note that a general non-collinear magnetic order is allowed.

Our search for the mean-field solution proceeds in two stages. First we assume the density to be uniform and perform an unrestricted search of the parameters  $\chi_{ij}$ ,  $\Delta_{ij}$  and  $\mathbf{m}_i$  (over  $6 \times 6$  elementary unit cells in a large lattice). For  $x < x_c$  we find  $\chi_{ij}$  to be a real constant as long as  $x$  is nonzero and  $\Delta_{ij} = 0$  while the spins form the  $\sqrt{3} \times \sqrt{3}$  non-collinear structure identified by Huse and Elser[11] for  $x = 0$ . If we denote the lattice by  $\mathbf{r}_i = n\mathbf{a} + l\mathbf{b}$ ,  $\mathbf{a} = \hat{x}$  and  $\mathbf{b} = -\frac{1}{2}\hat{x} + \frac{\sqrt{3}}{2}\hat{y}$ , then a representative solution has  $m_i^z = 0$  and  $m_i^x + im_i^y = |\mathbf{m}|e^{i\mathbf{Q} \cdot \mathbf{r}_i}$ , where  $\mathbf{Q} = (2\pi/3, 2\pi/\sqrt{3})$  and  $\mathbf{Q} \cdot \mathbf{r}_i = \frac{2\pi}{3}(n+l)$ .  $|\mathbf{m}| = \frac{1}{2}$  at zero doping, and decreases gradually with increasing doping. It is roughly  $0.35 \sim 0.38$  (depending on our choices of  $t/J$ ) at  $x = x_c$ , where the long-range ordered magnetic state undergoes a first order phase transition into a uniform  $d_{x^2-y^2} \pm id_{xy}$  superconducting state. The value of  $x_c$  is 3.8%, 3.7%, 2.2%, 2.1% for  $t/J = 5, -5, 9, -9$  respectively. Even if the pairing channel is removed, the magnetic order extends only up to  $x_* = 4.5\%, 4.2\%, 2.4\%, 2.4\%$  for the same set of  $t/J$ . This is significantly different from the mean-field solution of the square lattice with  $t/J = 3$  as appropriate for the cuprates. In that case the system is inhomogeneous with alternating stripes of superconducting and magnetic regions at roughly  $2\% \leq x \leq 12\%$ , and the magnetic order becomes commensurate with coexisting uniform pairing order at higher doping levels up to  $x_c \sim 20\%$ . [12] For the hexagonal lattice, the stable region of the anti-ferromagnetic solution is greatly reduced. This is reasonable in view of the frustration of the lattice, which disfavors magnetic order and was the original motivation of the RVB as a competing state[2].

In the second stage of the calculation we concentrate on doping greater than  $x_c$ . In view of the first-order nature of the transition to magnetic order, we shall present results without magnetic order even for  $x < x_c$ , with the understanding that the solution is only locally but not globally stable. We suppress magnetic order and perform an unrestricted search for solutions of  $H_{nm}$  in Eq. (4) on a  $400 \times 400$  lattice. In the elementary unit cell (varied from  $1 \times 1$  up to  $4 \times 8$ ) we put random initial values for  $\chi_{ij}$ ,  $\Delta_{ij}$ ,  $x_i$  and  $\mu_i$ , and evolve them so that the mean-field free energy is minimized at the desired doping level. Note that this time we allow nonuniform charge density. However, with our choice of parameters, we found spatially non-uniform solutions only for  $x < x_u$ , where  $x_u$  is always less than  $x_c$  and these will be ignored from now on. Due to the uncertainty of  $t/J$  we have studied two cases  $|t/J| = 5$  and  $|t/J| = 9$ . It turns out that in both cases there is a significant doping range in which the ground state is superconducting. The pairing symmetry is always  $d_{x^2-y^2} + id_{xy}$ , hence breaks the time reversal symmetry. It is interesting to note that if one ignores the magnetic order parameter at zero doping the same mean-field theory predicts a degenerate family of ground states. Among them the  $d_{x^2-y^2} + id_{xy}$  paired state and the  $\pi/2$  flux state are two examples.[13, 14] To visualize the pairing pattern, consider an arbitrary site. The  $\Delta_{ij}$  associated with the six bonds stemming from it has the form  $\Delta_{ij} = \Delta e^{i2\theta_{ij}}$  for  $d_{x^2-y^2} + id_{xy}$  pairing and  $\Delta_{ij} = \Delta e^{-i2\theta_{ij}}$  for  $d_{x^2-y^2} - id_{xy}$  pairing. To generate the pairing field over the entire lattice, simply translate the above pattern to other sites. In the absence of a magnetic field the  $d_{x^2-y^2} + id_{xy}$  and  $d_{x^2-y^2} - id_{xy}$  pairing are degenerate.

The doping dependence of the zero temperature pairing order parameter  $\Delta = |\Delta_{ij}|$  is plotted in Figs.2 (solid lines) for  $t = 5J$  (a),  $9J$  (b),  $-5J$  (c), and  $-9J$  (d), where we observe that pairing exists for  $x \leq 13\%$  (a), 8% (b), 56% (c) and 13% (d). The peak in  $\Delta$  at  $x = 0.5$  in Fig.2(c) is explained by the Van Hove peak in the free electron density of states. Also shown in Figs.2 is the hopping order parameter  $\chi = |\chi_{ij}|$  (dashed lines). It is weakly dependent on  $x$  for  $x < 30\%$ . Interestingly  $\chi_{ij}$  has the same sign of  $t$  from our calculation. This is a reasonable result as it increases the band width of the fermions so that the kinetic energy is lowered. Finally, a much more important feature in Figs.2 is the considerable asymmetry between electron doping ( $t > 0$ ) and hole doping ( $t < 0$ ). This is due to the particle-hole asymmetry in the free-electron dispersion on the triangular lattice. Indeed, the stronger pairing for hole doping is due to the increases in the Fermi level density of state as the averaged occupation decreases from half-filling.

We have also computed the onset temperature of the RVB fermion pairing and Bose-Einstein condensation (BEC) of holons.[15] The mean-field superconducting transition is the smaller of the RVB and BEC curves

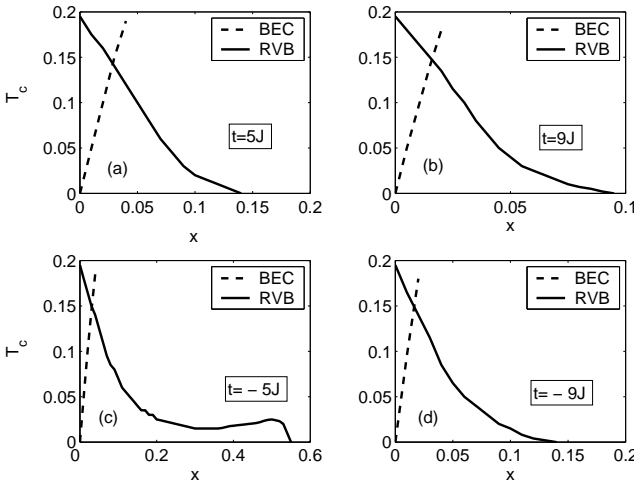


FIG. 3: Dependence of the RVB and BEC critical temperatures (in units of  $J$ ) on hole doping ( $x$ ):  $t = 5J$  (a),  $9J$  (b),  $-5J$  (c), and  $-9J$  (d). Note the scale change in 2(b) and 2(c).

(Figs.3). As usual, the Bose condensation temperature is an overestimate of the phase coherence temperature of the slave bosons. More generally because of the proximity to the Mott insulator limit, we expect that the superconducting transition temperature will be determined by the superfluid density at low doping, and by the onset of pairing at higher doping, forming a phase diagram similar to that of the cuprates. It is worth noting that in the case of cuprates, the thermal excitation of nodal quasi-particles significantly reduces the superfluid density and therefore the transition temperature at low doping.[16, 17] The existence of a full gap in the  $d_{x^2-y^2} + id_{xy}$  state suppresses this possibility and everything else being equal, we can expect a higher  $T_c$  in this case.

We conclude that within the slave boson mean field theory, the system exhibits non-collinear antiferromagnetism for  $x < x_c$ . Above this lower critical concentration and below certain upper critical concentration the system exhibits time reversal symmetry breaking  $d_{x^2-y^2} + id_{xy}$  pairing state. The orbital moment produces a magnetic field which can be detected by  $\mu$ SR. The field has been estimated to be 15 Gauss for the anyon model [18] but a calculation based on the slave boson mean field theory yields a smaller estimate of 1 Gauss near a vacancy. [19] If the orbital moment in neighboring layers are parallel, this state has been predicted to exhibit fascinating new effects such as quantized spin Hall conductance and anomalous Hall thermal conductivity.[20] The orbital moment corresponds to roughly  $\frac{1}{20}\mu_B$ , and field cooling in a modest magnetic field may line up the orbital moments. It will clearly be desirable to achieve such a state in the laboratory. For  $|t/J| = 5$  ( $|t/J| = 9$ ), the  $d_{x^2-y^2} + id_{xy}$  superconductor is expected to exist over a low doping

range  $x < 13\%$  ( $x < 8\%$ ) for electron doping, and a wider range  $x < 56\%$  ( $x < 13\%$ ) for hole doping. Thus some ingredient in addition to the t-J model may be needed to explain the experimental observation of superconductivity at  $x = 0.35$  in electron-doped  $\text{Na}_x\text{CoO}_2 \cdot y\text{H}_2\text{O}$ . Exploration of the  $\text{Na}_{1-x}\text{TiO}_2$  system may be more promising. We also note that  $\text{Na}_{0.7}\text{CoO}_2$  is a metal which exhibits unusual behavior such as linear  $T$  resistivity and large magnetic-field-dependent thermal power.[21] This is also inconsistent with the mean field prediction of Fermi liquid in the overdoped region, suggesting that some additional physics may be at work. In any event, the new observation opens up the possibility of changing the doping concentration in a controlled way by intercalation and much new physics surely remains to be discovered.

After the completion of this work we have seen a paper by Kumar and Shastry [22] reaching similar conclusions. However, we do not agree with their identification of the sign of  $t$ .

We thank Fangcheng Chou, Joel Moore, T.K. Ng, and N.P. Ong for helpful discussions. QHW is supported by NSFC 10204011 and 10021001, and by the Ministry of Science and Technology of China (NKBRSPF-G1999064602). He also thanks Z. D. Wang for hospitality in the University of Hong Kong. DHL is supported by DOE grant DE-AC03-76SF00098. PAL is supported by NSF DMR-0201069. He also thanks the Miller Institute at Berkeley for support.

---

- [1] J.G. Bednorz and K.A. Müller, *Z. Phys. B* **64**, 189 (1986).
- [2] P.W. Anderson, *Science* **235**, 1196 (1987).
- [3] K. Takada, H. Sakurai, E. Takayama-Muromachi, F. Izumi, R. A. Dilanian, and T. Sasaki, *Nature* **422**, 53 (2003).
- [4] G. Baskaran, [cond-mat/0303649](http://arxiv.org/abs/cond-mat/0303649).
- [5] S. Yu. Ezhov, V.I. Anisimov, H.F. Pen, D.I. Khomskii, and G.A. Sawatzky, *Europhys. Lett.* **44**, 491 (1998).
- [6] D. J. Singh, *Phys. Rev. B* **61**, 13397 (2000).
- [7] T. Valla, P. D. Johnson, Z. Yusof, B. Wells, Q. Li, S. M. Loureiro, R. J. Cava, M. Mikami, Y. Mori, M. Yoshimura, and T. Sasaki, *Nature* **417**, 627 (2002).
- [8] A. Seidel, C. A. Marianetti, F. C. Chou, G. Ceder, and P. A. Lee, *Phys. Rev. B* **67**, 020405 (2003).
- [9] S. J. Clarke, A. C. Duggan, A. J. Fowkes, A. Harrison, R. M. Ibberson, and M. J. Rosseinsky, *Chem. Commun.* **1196**, 409 (1996).
- [10] J. Brinckmann and P.A. Lee, *Phys. Rev. B* **65**, 014502 (2001).
- [11] D. A. Huse and V. Elser, *Phys. Rev. Lett.* **60**, 2531 (1988).
- [12] Jung Hoon Han, Qiang-Hua Wang and Dung-Hai Lee, *Int. J. Mod. Phys. B* **15**, 1117 (2001).
- [13] V. Kalmeyer and R. B. Laughlin, *Phys. Rev. Lett.* **59**, 2095 (1987).
- [14] T.K. Lee and S. Feng, *Phys. Rev. B* **41**, 11110 (1990).
- [15] For BEC calculation, an artificial tiny dispersion in the

z-direction is needed. See, e.g., G. Kotliar and J. Liu, Phys. Rev. B **38**, 5142 (1988).

[16] P.A. Lee and X.-G. Wen, Phys. Rev. Lett. **78**, 4111 (1997).

[17] J. Corson, R. Mallozzi, J. Orenstein, J. N. Eckstein, and I. Bozovic, Nature **398**, 221 (1999).

[18] B.I. Halperin, J. March-Russell and F. Wilczek, Phys. Rev. B **40**, 8726 (1989).

[19] B. Braunecker, P. A. Lee and Ziqiang Wang, to be published.

[20] T. Senthil, J.B. Marston and M.P.A. Fisher, Phys. Rev. B **60** 4245,(1999).

[21] I. Terasaki, Y. Sasago and K. Uchinokura, Phys. Rev. B **56**, 12685 (1997); Y. Y. Wang, N. S. Rogado, R. J. Cava, and N. P. Ong, Nature **423**, 425 (2003).

[22] B. Kumar and B.S. Shastry, cond-mat/0304210.